DI-9 # Cyclic Strain and Fatigue Behavior of Metals in the Creep Range

L. F. Coffin, Jr. *

Abstract

In this report the problem of the resistance of metals to low cycle fatigue at elevated temperature is considered. This problem is of considerable importance in the design for finite life of a wide range of machines, devices and components such as turbomachines, pressure vessels, fuel elements, etc. The approach followed is to develop a relationship between equivalent ductility, ϵ_f', and a parameter $P_1=f(\dot{\epsilon}_p,T)$ such that for particular strain rates and temperature the fatigue life can be determined from the well-known low cycle fatigue equation $N_f^{1/2}\,\Delta\epsilon_p = \epsilon_f'/2$. Support for this approach is obtained from experiments on a 0.1%C, 2.0%Mo steel over a wide range of temperature and strain rates. It is proposed that construction of parametric curves for other steels in the creep range can be made from constant strain rate to fracture tensile tests. The general validity of the approach requires much further experimental support than exists to date.

*
General Electric Research and Development Center
Schenectady, New York

Introduction

A considerable amount of work had been undertaken to study the behavior of ductile metals subjected to controlled cyclic plastic strain, both as a problem in deformation and in fracture (1). From this work there has evolved a quite simple, straightforward criterion for fatigue fracture, which has proved useful as the source for material response in the design of pressure vessels for nuclear application and of other structures (2,3). This had lead to a much more sophisticated design basis for nuclear pressure vessels such that by following certain design rules (2) finite cyclic life can be accounted for. An important restriction to this procedure exists, however, in that the basic material information from which predictions of finite fatigue life can be made is limited to temperatures below the creep range. The presence of thermally activated processes is known to introduce complications to the plastic deformation of metals so as to make the present low temperature design procedures unreliable.

It can be expected that consideration of elevated temperatures in engineering structures introduces many complications to the metals employed because of the increased thermal activity. On the other hand, most of the important problems in low cycle fatigue occur in this region. This is because the severe loading conditions which require limited life fatigue design most often arise from severe thermal stresses resulting from temperature transients, thermal mismatch or temperature gradients. Many examples can be cited in the design of steam and gas turbines, nuclear components such as core structures and fuel elements, heat transfer equipment, etc.

In the present paper the low cycle fatigue behavior of metals in the creep range is reviewed, including some very recent results. Based on this work, a method for treating the high temperature problem can be described and the necessary material information requirements determined. Generalizations of the method to broader applications are discussed.

Low Temperature, Low Cycle Fatigue Behavior

Much of the work which has been done in determining the behavior of ductile metals under conditions where time and temperature effects can be neglected was reviewed sometime ago (1). In this work tests were performed

to obtain information on metal behavior where strain, not stress, is the independent variable. Here the total strain range $\Delta\varepsilon$ can be broken down into elastic and plastic components. The plastic strain range $\Delta\varepsilon_p$ has been found to be an extremely important variable in plotting and predicting low cycle fatigue behavior. By representing the fatigue behavior of a particular metal in terms of the log $\Delta\varepsilon_p$ vs log N_f, where N_f is the number of cycles required for failure, a straight line is obtained over the entire range of the tests, whose slope is -1/2, regardless of the metal tested. Figure 1 is typical of the results found for many metals. Another point of interest is that the fracture ductility in simple tension, ε_f, can be represented on this figure if one considers that $\Delta\varepsilon_p = \varepsilon_f$ at $N_f = 1/4$ cycle. In this matter the fracture ductility ε_f is defined as

$$\varepsilon_f = \log_e \frac{A_o}{A_f} \qquad (1)$$

where A_o is the initial specimen area and A_f is the fracture area. The representative given by Fig. 1 can be expressed mathematically as

$$N_f^{1/2}\,\Delta\varepsilon_p = C \qquad (2)$$

but since $\Delta\varepsilon_p = \varepsilon_f$ at $N_f = 1/4$, $C = \frac{\varepsilon_f}{2}$. Thus the complete low cycle fatigue behavior can be determined from the fracture ductility of the metal, an extremely useful fact.

While Eq. 2 is of value for representation of fatigue data, it is not in a form useful for design. Designers use elastic stress analysis in determining the relationship of service conditions to material behavior. It is possible under many conditions to convert Eq. 2 to a form more adaptable to elastic design (2,3). Here the assumption is made that, despite the fact that the structure in question may undergo some plastic deformation due to external loads or thermal effects, elastic stress analysis can be applied to determine the strains so produced. When this procedure is followed, it can be shown that in many cases the strains, but not the stresses, so calculated are in good approximation to those actually obtained (4,5). These strains can be related to material behavior for design purposes. To determine the appropriate material information, it has been shown (2,3) that the relationship

$$\sigma_a = \frac{E\varepsilon_f}{4\sqrt{N_f}} + \sigma_e \qquad (3)$$

can be derived from equation 2. Here σ_a is the stress amplitude relatable to design analysis and σ_e the endurance limit. An alternate approach to the development of a design equation has been given by Manson and co-workers (6).

High Temperature Low Cycle Fatigue Behavior

As pointed out, a significant difference can be expected in the resistance of metals to cyclic plastic strain when elevated temperatures are employed. Here time and temperature become significant, and both of these variables must be carefully accounted for in failure interpretation. To put this into proper context, some early work on the low cycle fatigue resistance of lead is of interest. Figure 2 presents the data of Eckel (7) and Gohn and Ellis (8) for acid lead at slightly elevated temperature, in which the frequency of cycling is varied. Converting the data to the $\Delta\epsilon_p$-N representation, we find a strong frequency effect. In particular, if the low cycle fatigue relation is presented in the form

$$N^k \quad \Delta\epsilon_p = C \tag{4}$$

as proposed by Manson (9), and Coffin (10), the exponent k is strongly frequency dependent. Further, as the frequency is lowered, the fracture was observed to shift from transcrystalline to intergranular in character, further illustrating that high-temperature effects are operative. The reduction in fatigue life with decreasing frequency is most striking.

Although there are several investigations of the low cycle fatigue resistance at elevated temperature, Eckel's work is one of the few exceptions where the rate effects are considered. Swindeman (11) has reported the results of cyclic strain tests on Inconel at 1500°F at frequencies of 1 and 6 cycles per hour which also confirm equation 4, where C is approximately $\epsilon_f/2$ but where $k>0.5$ and increases with decreasing frequency.

Related tests have been reported by Walker (12) in which completely reversed, uniaxial cyclic strain tests were conducted on a cast 1%Mo, 1%Cr-1%Mo, 12%Cr-0.5%Mo and a AISI type 316 austenitic steels at 950°F in which hold times of varying magnitude were introduced. The results also showed a value of k in equation 4 in excess of 0.5, the amount depending on the particular material considered.

Another way in which cyclic plastic strain is produced in metals is by repeated temperature cycling accompanied by mechanical constraint. Indeed much of the interest in low cycle fatigue arises from this type of loading, the phenomenon being referred to as thermal fatigue or thermal stress fatigue. For example, craze cracking in rolls, molds, dies, and the like is a consequence of cyclic biaxial thermal stresses produced when a metal surface undergoes large thermal fluctuations while the interior of the part remains at fairly constant temperature. The phenomenon of craze cracking has been thoroughly studied by Northcott and Baron (13).

Interpretation of the fatigue resistance of metals to this type of loading is complicated by the level of temperature generally encountered, by the range of the temperature cycles, and by time. It is necessary therefore to take these additional variables into account before any generalizations are made regarding thermal fatigue.

In a comprehensive study of AISI type 347 stainless steel subjected to cyclic thermal stress (10), many of the observations described earlier regarding the deformation and fracture resistance of metals at low temperature apply. These include cyclic strain hardening and softening and the verification of Eq. 2. Fig. 3 is included to show the similarity. It will be noted that the mean temperature in these tests was 350°C, a temperature too low for appreciable time-dependent effects. Other comparisons of thermal and mechanical strain cycling has been made by Majors (14), Kennedy (15) and Carden (16). Comparison of mechanical and thermal cycling tests on Hastelloy N, taken from reference 16 are shown in Fig. 4, confirming equation 4.

Other investigators have found that the maximum temperature is an important variable in the materials and test conditions they employed. Clauss and Freeman (17) have studied this question thoroughly for alloys S-816 and Inconel 550 using temperatures as high as 1600°F. They found that the cycles to failure were more sensitive to changes in the maximum temperature of the cycle than the temperature range. Fig. 5 taken from that study shows this behavior somewhat differently indicating that at the lower temperatures equation 2 does indeed hold, in agreement with the stainless steel investigation (10), but at higher temperatures k = 2.0 or more. Similar findings have been reported by other investigators (18, 19).

Thus time-dependent effects which can influence the deformation and fracture resistance of the metal play an important role in low cycle fatigue. Time and temperature generally bear some functional relationship; hence frequency of cycling and hold time at temperature should have the same effect as a change in temperature. Thus it is not surprising to find the results indicated from Fig. 2 for lead, and Fig. 5 for S-816 to be in the same direction regarding the exponent k.

Information regarding the effect of frequency and hold time, found to be so important in the case of lead (Fig. 2) is very sparse for structura metals at elevated temperatures. Increasing the length of the hold time in the thermal cycling of 347 stainless steel decreases the life (10), while decreasing the frequency of cycling of Inconel at 1300° to 1650°F increases k and decreases the life (20).

Montonic Deformation and Fracture of Low Alloy Steels at Elevated Temperature

We turn now to the consideration of some work on the effect of temperature on the deformation and fracture of low alloy steels under monotonic loading. Interest in this stems from the close relationship of low cycle fatigue to tensile fracture, and from the fact that low alloy steels are the most common material of construction for nuclear pressure vessels.

The work of Glen is of considerable interest, particularly in regard to the effect of various alloying additions on the true stress-strain curve and on fracture ductility at various elevated temperatures and constant strain rate. He has shown that strain-age hardening occurred during plastic straining, which was quite specific both to the temperature of the test and to the alloying element involved (21,22). When strain-age hardening was noted at a particular temperature, a minimum on reduction of area was also obtained. Provided the temperature for the minimum reduction of area exceeded 300°C, all minimum ductility fractures were found to be intercrystalline in nature.

Fig. 6 summarizes some of his work for various steels, both with respect to the stress level reached in the tension test after straining to 10%, and the reduction in area. For the carbon steels containing molybdenum, two minimum in reduction of area were noted, one occurring at 200-250°C, depending on the percentage of molybdenum in the alloy, and at 600°C. The lower ductility minimum was attributed to a dislocation-induced precipitate of carbon adjacent to molybdenum atoms, associated with an increase in solubility of carbon and nitrogen in ferrite due to the presence of molybdenum. At 600°C, molybdenum diffuses readily and precipitation of Mo_2C occurs preferably on dislocation sites, accounting for the strengthening and the ductility minimum at this temperature.

Glen has investigated these effects not only in short time tensile testing, described above, but also in creep. He has shown (23) that strain-age hardening in constant stress creep tests leads to transitions in the creep rates as manifested by sudden deceleration in creep over an interval of time. These transitions are most clearly seen in so-called "strain/rate" curves which are plots of creep tests in which the logarithm of the instantaneous creep rate is plotted against the logarithm of total plastic strain accumulated at any point in time of the test. Results of the effects of alloying elements such as nitrogen, carbon, manganese, chromium, molybdenum, vanadium, titanium and silicon on these curves support this position.

Fatigue Behavior of a Low Carbon Steel at Elevated Temperature

In two recent papers we have shown that cyclic strain aging plays an important role in the cyclic strain and fatigue behavior of mild steel (24,25). One steel considered was SAE1111, tested in both the annealed condition and with an ice brine quench from 675°C to increase the supersaturation of carbon in solution at room temperature. With respect to low cycle fatigue, a diametral strain range $\Delta\epsilon_d = .02$ and a cross head speed of 0.2 inches per minute were selected. Results are shown in Fig. 7 for annealed and ice-brine-quenched SAE1111 steel. The very striking influence of temperature for both heat treatments is noted, and in particular the decrease in life by a factor in excess of three between 150° and 250°C for the ice-brine-quenched steel can be seen. A minimum in fatigue life is found at 250°C for both thermal treatments.

The cycles-to-failure results can also be presented as a function of the plastic strain range. The three levels of the diametral strain range, $\Delta\epsilon_d$, namely, 0.015, 0.020 and 0.025, were employed at 150° and 250°C for the ice-brine-quenched SAE1111 steel. These results are shown in Fig. 8 together with more complete results for the annealed steel at room temperature and 200°C. Comparison with these more extensive tests reveals the quenched steel tested at 150°C to have a greater resistance and the 250°C tests to be considerably poorer than the annealed steel.

In addition to the above, tension tests were conducted on the steel at various temperatures with various thermal and mechanical pretreatments. These were done for two specific purposes. The first was to determine if the fracture ductility could be utilized to predict the marked influence of temperature on the fatigue resistance as shown in Fig. 7. As discussed above, there is considerable information (1) which shows that the fracture ductility (true strain at fracture) can be utilized to predict the low-cycle fatigue curve for many metals. The performance of the present steels would put this observation to a severe test. A further interest is the use of fracture ductility as a means of determining the effect of the several thermal and mechanical treatments on the subsequent low-temperature ductility. Since strain aging and quench aging are known to produce deleterious effects on the brittle-ductile transition temperature of steels, the effects of cyclic-strain aging on this phenomenon are of interest. While the standard Charpy notched bar is the commonly accepted means by which this behavior is investigated, that specimen shape did not lend itself to the present method of cyclic-strain aging. Instead, the fracture ductility of the simple tension test was used. The low-temperature tests were conducted in a variety of liquid baths, ranging through liquid nitrogen, liquid freon, and dry ice and alcohol.

Fig. 9 shows the relationship between fracture ductility and temperature for annealed SAE1111 over the range of -100° to 500°C for two different strain rates. Shown also for comparison purposes are ductility values computed from the fatigue results of Fig. 7. This is done by means of the relationship

$$\epsilon_f = 2 N_f^{1/2} \Delta\epsilon_p \qquad (5)$$

by substitution of the appropriate plastic-strain range and cycles to failure in (2).

The tensile transition temperature behavior of SAE1010 and 1111 steels with various thermal and mechanical pretreatments is shown on Fig. 10 wherein the annealed and quenched, then cyclic-strain-aged, conditions are compared. In addition, the effect ice-brine quenching is shown for SAE1111. For the case of cyclic-strain aging, a strain range of 0.02 diametral strain at 250°C for 10 cycles was employed. Subsequently, 10 mils of specimen surface was removed by grinding prior to tension testing to eliminate the possible influence of surface cracking. An increase in the tensile transition temperature in excess of 100°C was obtained by the quenched and cyclic-strain-aged pretreatment for both steels. Notched bar and nil ductility transition temperatures well in excess of room temperature would be expected for the steels in the quenched and cyclic-strain-aged condition.

From these studies it is concluded that for this steel, the metallurgical changes which occur during cyclic straining have a pronounced influence on the behavior of the material both with regard to fatigue resistance and brittle fracture. Similar effects also occur for monotonic loading. Thus the work of Glen, reported earlier for various low alloy steels begins to take on added meaning, when considering cyclic strain.

<u>Low Cycle Fatigue Behavior of an Annealed 0.1%C-2.0%Mo Steel</u>

In another recent paper (26), the cyclic strain and fatigue behavior of a 0.1%C,-2.0%Mo steel was studied at various temperatures and strain rates under uniaxial push-pull loading. As seen from Fig. 6, the presence of molybdenum can produce considerable strengthening and loss of tensile ductility at temperatures near 600°C for monotonic deformation. Similar results were found under cyclic straining.

The number of cycles required for failure plotted as a function of testing temperature is shown in Figures 11 and 12. In Fig. 11 the strain range is considered as parameter, while in Fig. 12, the effect of strain rate is examined. In each case a precipitous decrease in fatigue resistance is observed at temperatures of 500°C and above, showing the strong effect of the aging reaction on cycles of strain prior to failure as well as on cyclic hardening. Both figures reveal the strong influence of temperature on fatigue life under conditions of controlled cyclic strain. Fig. 12 is of particular interest, since the sensitivity of fatigue life to strain rate appears to be particularly pronounced. Note for example, that 550°C, a crosshead speed of 0.2 inches per minute leads to failure after 100 cycles with a diametral strain range of 0.02. Decreasing the crosshead speed to 0.002 inches per minute for the same strain range lowers the fatigue life to nine cycles.

Fatigue fracture surfaces were examined in several cases. For tests at 500°C and below fractures were transcrystalline; in the region of precipitous drop in fatigue life, fracture surfaces were intercrystalline.

Tension tests at constant crosshead speed were conducted at several temperatures. Corrected to true stress and strain, the results are shown in Figures 13 and 14. In Fig. 13 temperature is the parameter, while in Fig. 14 the effect of crosshead speed is observed at 600°C. The aging reaction is seen to influence the shape of the curves, both with regard to flow stress and fracture. It is noted in particular that the fracture ductility decreases with increasing temperature, and with decreasing strain rate.

<u>A Parametric Approach to Low Cycle Fatigue at Elevated Temperature</u>

The role of rate effects on monotonic or cyclic loading of this alloy at elevated temperatures must be accounted for in any evaluation of fracture. As has been discussed earlier, the pronounced loss in ductility appears to be the result of a metallurgical reaction. Evidence provided by the present experiments and by the work of Glen (22) would indicate that the reaction involved here is the precipitation of Mo_2C on dislocations to form a coherent precipitate. It would appear that this one process alone is controlling with respect to ductility loss for the range of test conditions employed, and hence the effects involve a single activation energy. There is, then, the strong suggestion that strain rate or time and temperature can be combined into a single variable or parameter. Much has been written on the parametric approach to the creep problem and a number of parameters have been proposed, but the focus for this approach has been stress. For example, flow stress curves at constant strain levels have been represented by the so-called "velocity-modified temperature" (27), generalized creep curves have been formulated through the use of a strain rate (or time), activation energy, temperature parameter (28), and stress-rupture data has been represented by Larson-Miller (29), or Manson-Haferd type parameters (30). With but one possible exception, the question of ductility has been ignored in these considerations. This probably stems from the fact that ductility is not directly a design consideration for creep, and its use involves a qualitative judgment rather than a quantitative determination, as compared to stress.

However fracture ductility has direct design implications through the use of equation 2 and its extension to low cycle fatigue design at low temperatures (3). The existence of a quantitative relationship between fracture strain and temperature-time applicable to low-cycle fatigue prediction could significantly improve our ability to design at high temperature. Thus it would be of interest to examine the data from this viewpoint. Reference at this point can be made to the work of MacGregor and Fisher (27) on which tension tests were conducted on annealed SAE1020, and 1045 steel and on annealed 60-40 brass at constant true strain rates to fracture. Strain rate and temperature are combined by means of the velocity-modified temperature T_m. Although the emphasis was on the flow stress, fracture ductility was also represented by this parameter. The data showed the true strain at fracture to be a single valued function of T_m. Unfortunately strain rates were not varied over a sufficient range to reveal convincingly the uniqueness of T_m in describing the interplay between temperature and strain rate. Nevertheless this form of the parameter is of interest for the present experiments.

In the conduct of both the monotonic and cyclic tests on the molybdenum steel, crosshead speed, rather than true strain rate was maintained constant. In each instance the strain varied somewhat during the course of the experiment, and as a result, only average strain rates were employed in the evaluation of the parameter. These were determined from the measured true strains obtained from the start of the test to fracture divided by the time of the test, or from the plastic strain range divided by one-half of the average period, depending on whether the test was monotonic or cyclic.

To find a common basis for comparing cyclic and monotonic experiment, the fracture ductility is employed, defined as the true strain at fracture for the monotonic tests or an equivalent ductility as determined from equation 2 for cyclic tests. Thus for a particular cyclic strain experiment

$$\varepsilon_f' = 2N_f^{1/2}\,\Delta\varepsilon_p \tag{5}$$

where ε_f' is the equivalent ductility. To determine the parameter best representative of the data involving temperature and strain rate, the fracture and equivalent ductilities are first plotted against $\log_{10}\dot{\varepsilon}_p$ where $\dot{\varepsilon}_p$ is the plastic strain rate for the various temperatures involved. Then choosing a specific ductility (ε_f=.5 was used), the quantity $\frac{1}{T}$ was plotted versus $\log \dot{\varepsilon}_p\,_{\varepsilon_f=0.5}$. The constants of the best straight line fit to the data were then evaluated, such that the resulting parameter was

$$P_1 = T(7.95 - \log \dot{\varepsilon}_p) \tag{6}$$

where T is the absolute temperature in degrees Kelvin. Fig. 15 summarizes all of the test data, which involved temperatures from 400 to 650°C and average strain rates from .06 to 53 inches/inch/hour, and the best fit line drawn through the test points. It will be noted that there is considerable overlap in the ranges of temperature and strain rate to support the validity of the parametric approach. Of equal importance is the fact that the tensile ductility data fits into this representation.

Another parametric representation can be made, based on total time, following the form of the stress-rupture parameters. It became apparent, when using only time of straining, that the tension tests were quite distinct from the cyclic tests. To bring these two types of tests into a single parameter it was necessary to include in the total time the quantity one hour. Actually about fifteen minutes was the maximum length of time held at temperature prior to straining, such that the additional time has little physical meaning. This parameter assumes the form

$$P_2 = T(7.38 + \log t) \tag{7}$$

where t is the time in hours. The test data of ductility employing this parameter are shown in Fig. 16. The principal distinction between the two parameters appears to be the degree of the fit of the tensile ductility data to the cyclic results.

It is of interest to show how well the two parameters predict low cycle fatigue life. For this purpose the parameter P_1 or P_2 is computed for a particular test, according to equation 6 or 7, and the ductility determined from the solid line of Fig. 15 or 16. The ductility normalized plastic strain range is then computed for that test, and is plotted against the actual cycles to failure of that test. In Fig. 17 is shown the comparison of these parametrically determined points to the relationship

$$N_f^{1/2} \frac{\Delta\varepsilon_p}{\varepsilon'_{f_p}} = 1/2 \qquad (8)$$

where ε'_{f_p} is either $\varepsilon'_{f_{P_1}}$ or $\varepsilon'_{f_{P_2}}$ as given from Fig. 15 or 16. All tests are included, and although agreement between experiment and prediction is satisfactory for both parameters, the strain rate parameter P_1 shows less scatter.

Relationship Between Cyclic Plastic Strain and Creep

From the evidence presented above for the 0.1%C, 2.0%Mo steel certain generalities can be drawn with respect to the general class of low alloy steels possessing elevated temperature strength. Following the position taken by Glen (22), strain-age hardening effects are largely responsible for the resistance to deformation for these alloys at elevated temperatures. Additions of carbon, nitrogen, manganese, molybdenum and chromium are the principal additives employed, the effectiveness of these additions in strengthening depending on the degree to which they are in solid solution prior to deformation at elevated temperature. To increase creep resistance these alloys are generally used in their normalized condition, whereby the cooling rates are such as to increase the degree of supersaturation of the alloy additions prior to use.

From the evidence presented in the above tests, and from the work of Glen, precipitate formation is accentuated by the combination of temperature and plastic strain as compared to strain alone. It is clear that these effects are beneficial if the objective is to retard plastic flow at elevated temperature, i.e., to develop creep resistance. On the other hand, when the component is subject to controlled cyclic plastic strain, these strain-induced reactions are "forced" to occur. Thus it is possible for cyclic plastic strain to be the major cause for premature failure. While a creep strain of 1% may be considered excessive in many cases, a much smaller but unaccounted for cyclic plastic strain occurring many hundreds of times, can in fact limit the service performance of the

component. There is an essential incompatibility in material selection between creep resistance and low cycle fatigue resistance. Optimization of alloy composition and heat treatment ot maximize creep resistance minimizes low cycle fatigue resistance, maximizing ductility for low cycle fatigue capacity reduces the ability of the metal to withstand steady stresses at elevated temperature.

Bases for Construction of Parametric Representation of Equivalent Ductility

From Fig. 15 and equation 6, prediction of low cycle fatigue resistance can be made for a specific temperature and strain rate. It was pointed out above that ductility information from both monotonic tension and low cycle fatigue tests gave identical results when plotted versus the parametric P_1. The question then arises as to how similar curves can be constructed for other alloys with various heat treatments. Various suggestions come to mind. One possibility is to utilize the rupture ductility as determined from the reduction in area, since a large volume of this data has been accumulated for a wide variety of metals over the past twenty-five years. Some reflection will reveal that these tests do not supply the necessary information. In a rupture test which is conducted under constant load, the strain rate in the deforming portions of the specimen varies considerably during the course of the test. In particular, the development of a neck in the gage length increases the stress and the strain rate in an unstable manner. Since a large percentage of the total deformation can occur in the necking process when the strain rate increases rapidly, it is difficult in any one test to attach a particular strain rate which has any meaning in relating strain rate and temperature to ductility.

Similar arguments can be made with respect to most tension tests of uniform gage length at constant crosshead speed. While the strain rate remains nearly constant prior to necking, as necking progresses, the deformation is localized to that region and the local strain rate increases rapidly. The longer the gage length for a given specimen diameter, the greater the strain localization, and the less the meaning of a single strain rate in correlating the ductility with strain rate and temperature.

The correlation between cyclic strain tests and monotonic tension tests requires constant strain rate tension tests to fracture. Unfortunately very few tests of this type have been made, and, in fact, the only information which the author has found is that of MacGregor and Fisher (27) as discussed above. To construct Fig. 15 with assurance, an adequate selection of strain rates are required to provide overlap between results at the different temperatures employed.

Application of the Parametric Approach to Various Types of Cyclic Loading

In the experiments reported above, a plot of strain versus time gives a sawtooth waveform, the slope of which is of equal magnitude in forward and reverse loading. When the strain range is varied, the slope and hence the strain rate remains constant. The frequency changes with strain range such that

$$\omega = \frac{\dot{\varepsilon}_p}{2\Delta\varepsilon_p} \tag{9}$$

If tests are conducted at constant frequency and temperature, while the plastic strain range is varied from test to test, it is apparent that the strain rate decreases with decreasing strain range. Thus when constant frequency cyclic strain tests are made at temperatures and strain rates where thermally activated processes influence the behavior, as typified by Fig. 15, it would not be expected that equation 2 would be operative, because of the changing ductility with temperature and strain rate. It is possible to make a quantitative prediction of the relationship between plastic strain range and cycles to failure at elevated temperatures and various frequencies for the 0.1%C, 2.0%Mo steel from Fig. 15 and equation 6. The results are shown in Fig. 18 at a temperature of 500°C for frequencies ranging from 0.1 to 10,000 cycles per hour. The procedure is to first select a frequency, such that for various plastic strain ranges, the plastic strain rates are determined from equation 9. From these values and the test temperature, the parameter P is found for each case, and with the aid of Fig. 15 the appropriate equivalent ductility is obtained. Finally the fatigue life is obtained, using this equivalent ductility and the plastic strain range in equation 2. Note in Fig. 18 that decreasing frequency has the effect of increasing the slope of N_f vs $\Delta\varepsilon_p$, supporting the generally observed behavior discussed in reference to equation 4, above.

To determine in a particular alloy whether the exponent k of equation 4 should exceed 1/2, for qualitative guidance reference to the reduction of area in stress rupture tests can be made. If, for equivalent temperatures and times in rupture and fatigue testing, the rupture ductility decreases, it can thus be expected that the exponent k in equation 4 will exceed 1/2. Because of the limitations of the rupture ductility as discussed above, a quantitative evaluation of the effect of the change in rupture ductility with time of test in determine the decrease in fatigue resistance is suspect. Nevertheless it can be expected that the greatest loss in low cycle fatigue resistance will occur in those alloys which suffer the greatest loss in rupture ductility.

A complete cycle of strain in any given location of a component in service may undergo a complex interaction of temperature and strain rate during the cycle. Thermal cycling, cycles involving long hold times, etc., are commonly experienced. Predictions of the fatigue left of such cycles from the curves of equivalent ductility versus $P_1(\dot{\varepsilon}_p, T)$ may be possible, by breaking down the complex cycle into elements involving constant temperature and strain rate, and assessing, based on the magnitude of cyclic plastic strain for each element of constant temperature and strain rate, the expected life following Fig. 15. Failure from the complex cycle can then be made by applying a cumulative damage criterion such as Miner's law. The procedure is as yet unverified, however.

Summary

In this paper the problem of the resistance of metals to low cycle fatigue at elevated temperature is considered. This problem is of considerable importance in the design for finite life of a wide range of machines, devices and components such as turbomachines, pressure vessels, fuel elements, etc. The approach followed is to develop a relationship between equivalent ductility, ε_f', and a parameter $P_1 = f(\dot{\varepsilon}_p, T)$ such that for particular strain rates and temperature the fatigue life can be determined from the well-known low cycle fatigue equation $N_f^{1/2}\Delta\varepsilon_p = \varepsilon_f'/2$. Support for this approach is obtained from experiments on a 0.1%C, 2.0%Mo steel over a wide range of temperature and strain rates. It is proposed that construction of parametric curves for other steels in the creep range can be made from constant strain rate to fracture tensile tests. The general validity of the approach requires much further experimental support than exists to date.

References

(1) Coffin, L.F. Jr., Applied Materials Research 1, No. 3, (1962) 129.

(2) Langer, B.F., Trans. ASME 84D, (1962) 389.

(3) Tavernelli, J.F. and Coffin, L.F. Jr., Trans. ASME 84D, (1962) 533.

(4) Manson, S.S., Machine Design (June, July 1960).

(5) Langer, B.F., Welding J. Res. Suppl., 37, 411S (1958).

(6) Manson, S.S. and Hirschberg, M.H., 10th Sagamore Army Materials Research Conference, August 1963.

(7) Eckel, J.F., Proc. ASTM, 51, 745 (1951).

(8) Gohn, G.R. and Ellis, W.C., Proc. ASTM, 51, 721 (1951).

(9) Manson, S.S., NACA Rept. 1170 (1954).

(10) Coffin, L.F. Jr., Trans. ASME, 76, 923 (1954).

(11) Swindeman, R.W., Joine International Conf. on Creep, Aug. 1963, paper 32.

(12) Walker, C.D., Joint International Conf. on Creep, Aug. 1963, paper 24.

(13) Northcott, L. and Baron, H.G., J. Iron Steel Inst., 184, 385 (1956).

(14) Majors, H. Jr., Trans. ASM, 51, 421 (1959).

(15) Kennedy, C.R., Proc. Fourth Sagamore Conf., Syracuse Univ. Res. Inst., 193 (1957).

(16) Carden, A.E., Paper No. 64 Met-2 ASME, 1964.

(17) Clauss, F.J. and Freeman, J.W., NACA TN-4160 (1958).

(18) Baron, H.G. and Bloomfield, B.S., J. Iron Steel Inst., 197, 223 (1961).

(19) Glenny, E., and Taylor, T.A., J. Inst. Metals, 88, II, 449 (1959-60).

(20) Swindeman, R.W. and Douglas, D.A., Trans. ASME 81D, 203 (1959).

(21) Glen, J., Amer. Soc. for Testing Materials, Spec. Tech. Publ 128, (1952) 184.

(22) Glen, J., J. of Iron and Steel Institute, 186, (1957) 21.

(23) Glen, J., J. of Iron and Steel Institute, 190, (1958) 114.

(24) Tavernelli, J.F. and Coffin, L.F., Jr., Proceedings of the Joint International Conference on Creep, ASME, Aug. 1963, paper 27.

(25) Coffin, L.F., Jr., General Electric Research Laboratory Report 64-RL-3550M, Jan. 1964. Also ASME paper 64-Met 8.

(26) Coffin, L.F., Jr., General Electric Research Laboratory Report 64-RL-3612M, March 1964, submitted for publication.

(27) MacGregor, C.W. and Fisher, J.C., Trans. ASME, 12, (1945), A-217.

(28) Orr, R.L., Sherby, O.D. and Dorn, J.F., Trans. ASM, 46, (1954) 113.

(29) Larson, F.R., and Miller, J., Trans. ASME, 74, (1952), 765.

(30) Manson, S.S. and Haferd, A.M., NACA Tech. Note 2890, (1953).

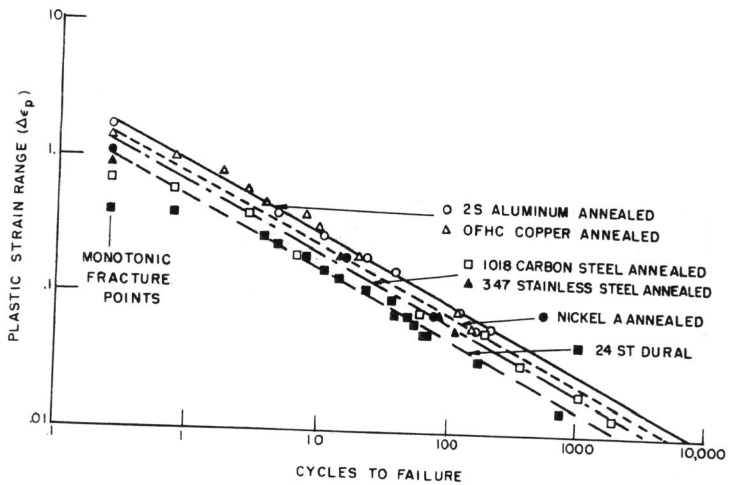

Fig. 1

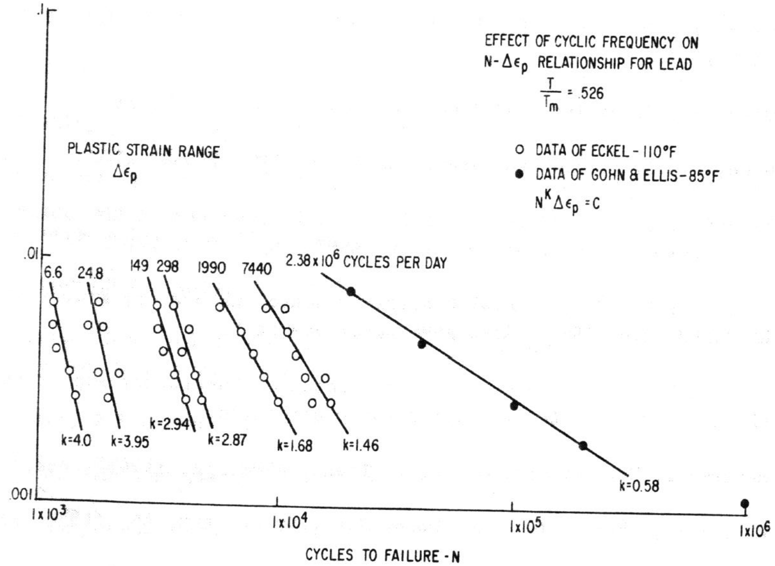

Fig. 2

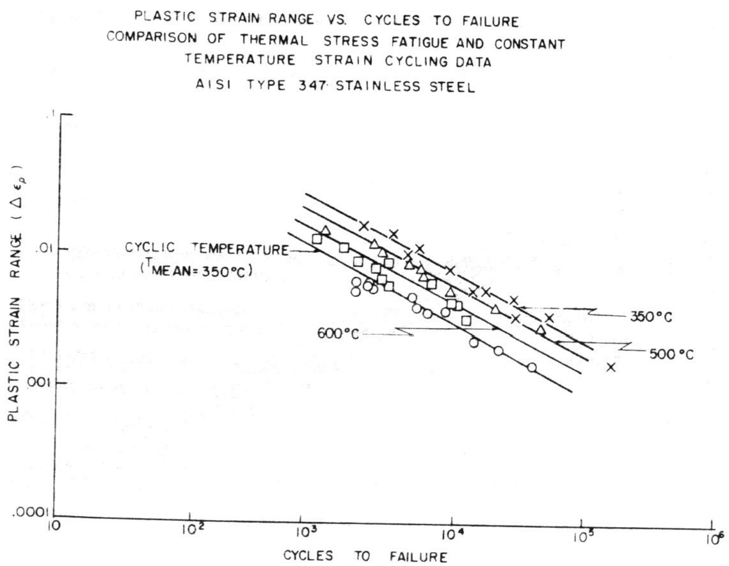

Fig. 3

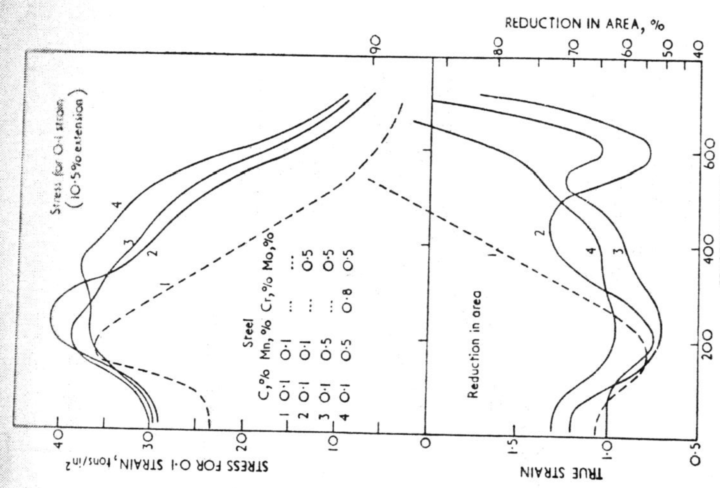

Fig. 6 Effect of Alloying Elements on the Flow Stress and Ductility of Low Alloy Steels (After Glen, Ref. 23).

Fig. 4

Plastic Strain Range vs Cycles to Failure for Hastelloy N.

Rectangular symbols for 1600°F maximum, thermal fatigue only.

Circular symbols for 1300°F maximum, open-thermal fatigue, solid-isothermal fatigue.

Triangular symbols for 1500°F, isothermal fatigue only. After Carden, Ref. 16.

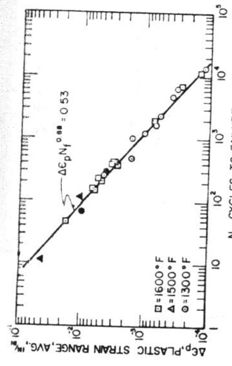

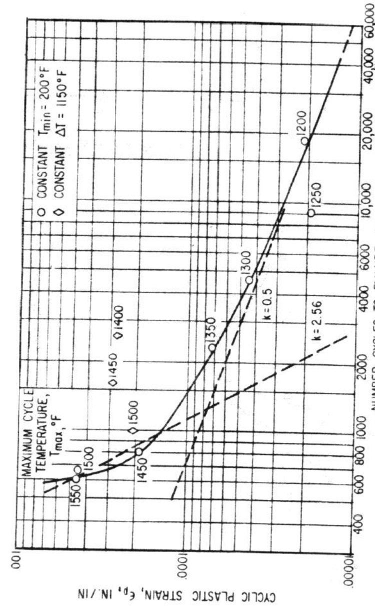

Fig. 5 VARIATION OF THE NUMBER OF CYCLES TO FAILURE S-816 SPECIMENS WITH THE AVERAGE PLASTIC STRAIN PER HALF CYCLE. HEAT OR COOL, 30 SECONDS; AT TEMPERATURE, 15 SECONDS (AFTER CLAUSS AND FREEMAN)

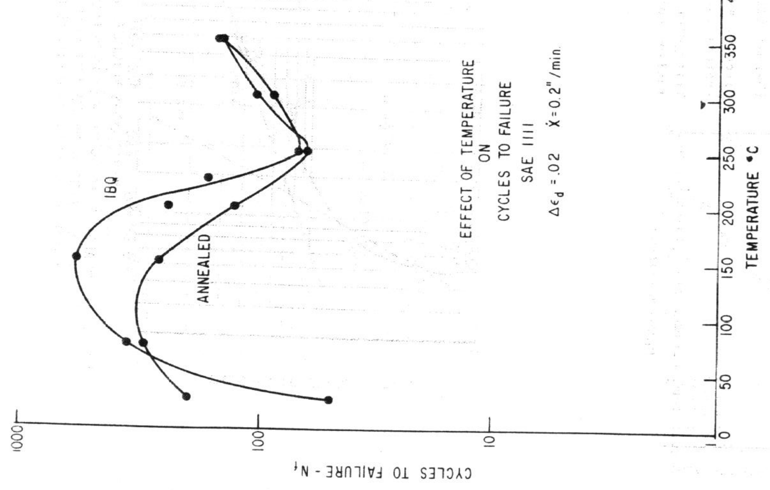

Fig. 7

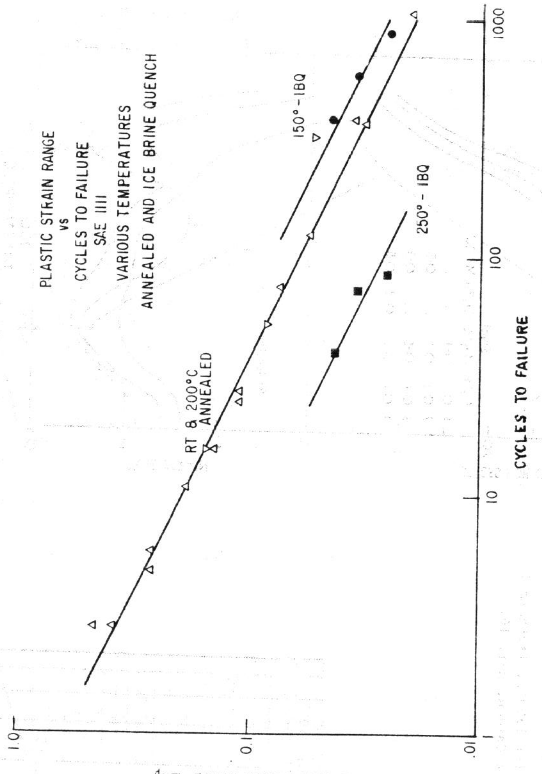

Fig. 8

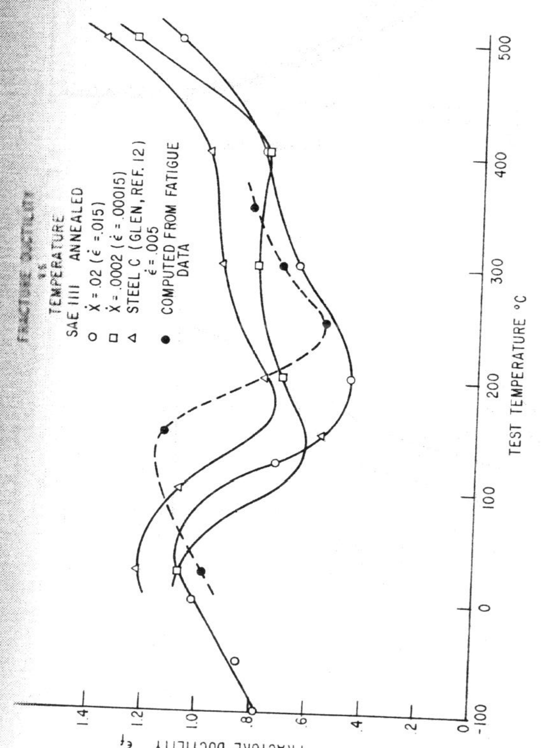

Fig. 9

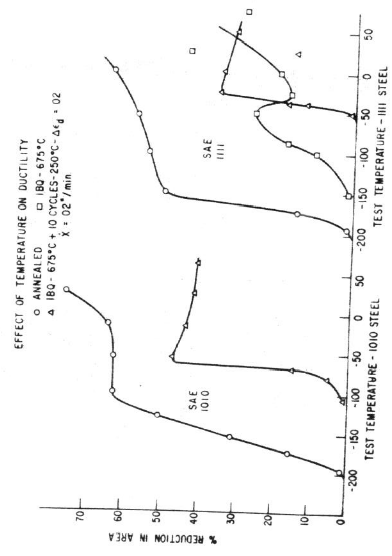

Fig. 10

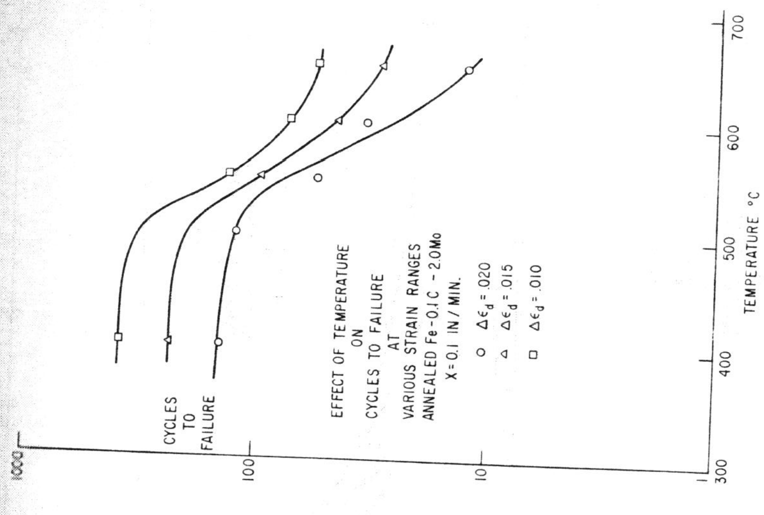

Fig. 11

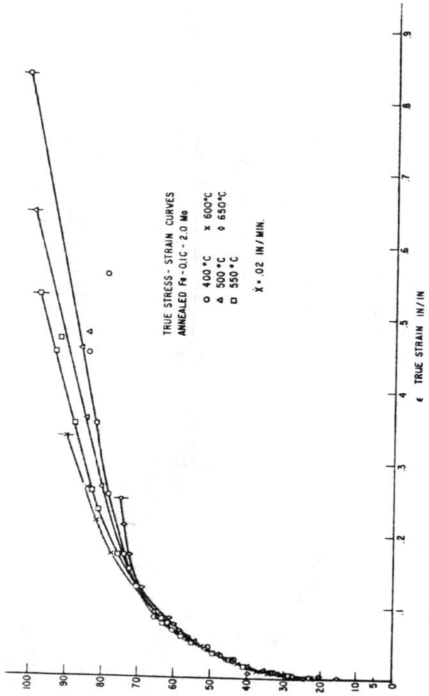

Fig. 13

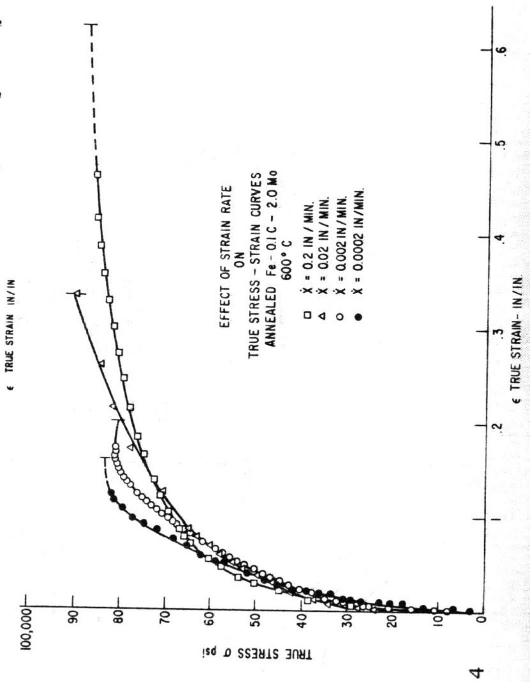

Fig. 14

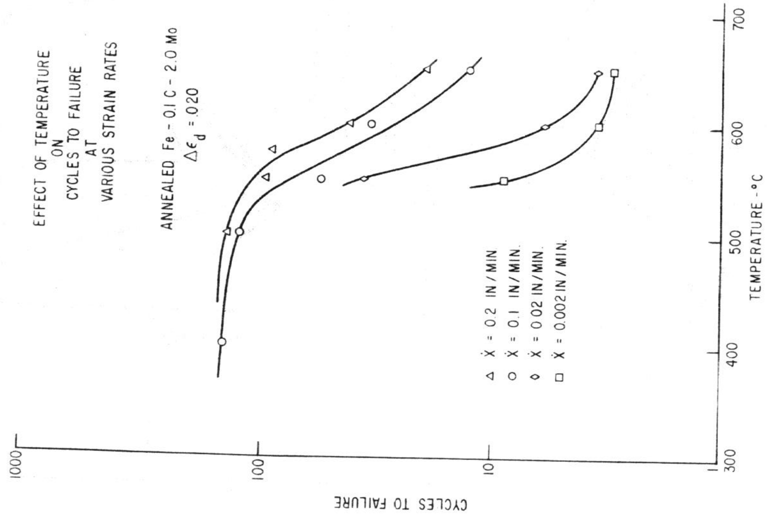

Fig. 12

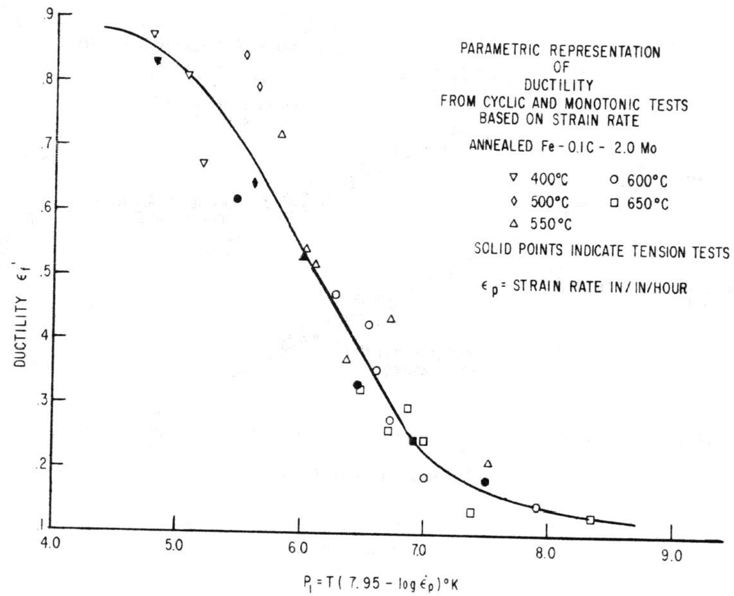

Fig. 15

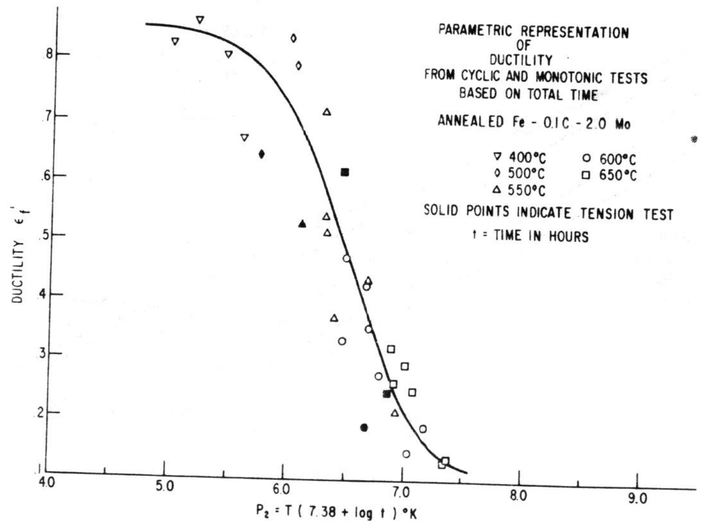

Fig. 16

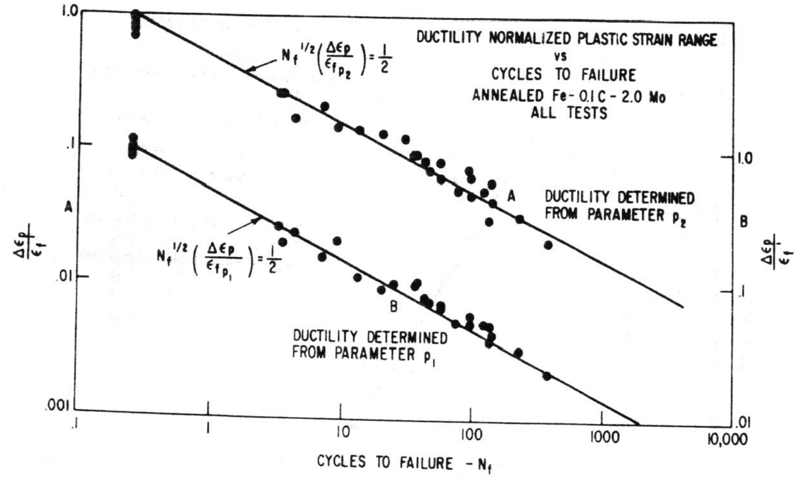
DUCTILITY NORMALIZED PLASTIC STRAIN RANGE
vs
CYCLES TO FAILURE
ANNEALED Fe-0.1C-2.0 Mo
ALL TESTS
DUCTILITY DETERMINED FROM PARAMETER p_2
DUCTILITY DETERMINED FROM PARAMETER p_1
$N_f^{1/2}\left(\frac{\Delta\epsilon_p}{\epsilon_{f p_2}}\right)=\frac{1}{2}$
$N_f^{1/2}\left(\frac{\Delta\epsilon_p}{\epsilon_{f p_1}}\right)=\frac{1}{2}$
A
B
$\frac{\Delta\epsilon_p}{\epsilon_f}$
CYCLES TO FAILURE - N_f

Fig. 17

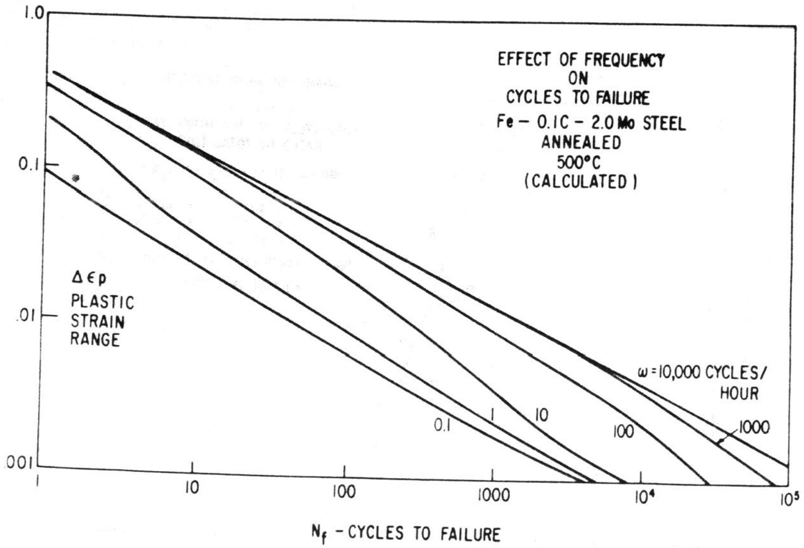
EFFECT OF FREQUENCY
ON
CYCLES TO FAILURE
Fe - 0.1C - 2.0 Mo STEEL
ANNEALED
500°C
(CALCULATED)
$\Delta\epsilon_p$
PLASTIC
STRAIN
RANGE
ω=10,000 CYCLES/
HOUR
1000
100
10
1
0.1
N_f - CYCLES TO FAILURE

Fig. 18